

Article - Engineering, Technology and Techniques

Saturation Approach for Dual-Band Transmission with Pre-Distortion for PA Efficiency Increase

Luis Schuartz^{1*}

<https://orcid.org/0000-0002-3202-1565>

Eduardo Lima¹

<https://orcid.org/0000-0001-6018-0128>

¹ Universidade Federal do Paraná (UFPR), Departamento de Engenharia Elétrica, Grupo de Circuitos Integrados e Sistemas (GICS), Curitiba, Paraná, Brasil.

Editor-in-Chief: Alexandre Rasi Aoki
Associate Editor: Alexandre Rasi Aoki

Received: 14-Jun-2023; Accepted: 30-Nov-2023

*Correspondence: luischuartz@ufpr.br; Tel.: +55-41-991998517 (L.S.).

HIGHLIGHTS

- Digital pre-distortion allows a concurrent dual band communication system to improve the efficiency guarantying the linearity.
- DPD saturation applied for dual band transmission improved the PA efficiency about 8 p.p.
- With DPD saturation for dual band transmission, the lost in EVM metric was less than 1 p.p.
- Sum and division approaches for dual band DPD saturation showed similar performances.

Abstract: Current wireless communication systems demand high data transmission throughput. To comply with this requirement, multiple concurrent communication channel usage are an option. The digital pre-distortion associated with the power amplifier (PA) in high suppression guarantees the linearity and maximum efficiency for a single transmission. However, reaching a high output transmission power using more than one band is not possible because the traditional pre-distortion cannot accept a saturation level. This work focuses on showing an approach for a dual-band transmission with an equivalent envelope saturation that, contrarily to previous dual-band crest factor reductions from literature based on only amplitude information, also takes into account the phase and frequency information. The introduced idea was tested by linearizing a broadband power amplifier for two-carrier, IEEE802.11n at 2.4 GHz and LTE at 3.5 GHz, concurrent transmission. Simulation results in the Cadence Virtuoso software showed gain of up to 8.8 percentage points (p.p.) in the PAE metric controlling with loss less than one p.p in EVM metric.

Keywords: Power amplifier; digital pre-distortion; concurrent transmission; efficiency; saturation.

INTRODUCTION

The main challenge for the current wireless communication systems is maintaining linearity, efficiency and high throughput simultaneously [1-6]. In the transmission system, the power amplifier (PA) is critical for linearity and efficiency due to its high DC power consumption and its non-linear behavior [7-8]. To operate in an efficient region the linearity is compromised, and to be linear the efficiency is compromised, which

generates a compromise between power efficiency and linearity [7,9]. The situation can be worsened for a high broadband PA because of the non-constant frequency behavior [10-11].

In a concurrent transmission, the usage of a single PA to operate in very broadband with more than one band simultaneously is desired to save power consumption. However, a treatment technique is mandatory [12]. The literature presents digital pre-distortion (DPD) as a good scalable and efficient way to transmission system linearization [5]. The DPD is a baseband block added to PA distortion compensation implementing a behavioral mathematical model [1,5,7], for example, polynomials from the Volterra series [13].

On the one hand, to achieve a high output data rate, the usage of multi-protocol and multiple communication channels is an option [14-15]. On the other hand, an efficient transmission system needs to operate with high power and attend to all communication systems. A PA with great broadband is an option that can attend this demand. Despite being efficient, the linearity of these transmitters is compromised due to the high transmission levels and nonlinear frequency PA behavior. In this case of concurrent band transmission, the digital pre-distorter (DPD) block, inserted in the baseband, can compensate accurately for the linearity of the transmitter [12]. However, the main problem of this approach is the limited output mean power, due to the distortion limit. For a single band, the DPD saturation is a recent option that allows increasing the transmitter output mean power controlling the distortions up to the standardization limits [16-17]. To attend to this demand, this manuscript introduces an approach of DPD saturation to dual-band transmission.

DPD implementation for current radio communication systems, as well as two-carrier transmission, are objects of recent research. References [22-24] contribute to dual-band DPD usage, as well as [25-28] approach peak-to-average power ratio (PAPR) problems for RF transmission. References [25] and [26] contribute with techniques for PAPR reduction applied for dual-band transmission. By on the one hand, [25] introduces an analysis of dual-band equivalent envelope and resumes it to the worst case, where the equivalent envelope is obtained using only amplitude information. On the other hand, [26] applies dual-band crest factor reduction (CFR) in a dual-band transmission with DPD implementation. But similar to [25], [26] used the PAPR in the worst case and the tests were done with carriers that are closed to each other.

This work contribution is a mathematical signal treatment that allows the traditional DPD, using the saturation procedure, to be applied for dual-band transmission. The approach of this manuscript is very similar to CFR, which has as its goal PAPR reduction. In this context, this work differs from [25,26] mainly in two aspects. First, the equivalent envelopes for both channels consider the phase and the frequency contributions. In other words, the equivalent envelope does not work in the worst case, which can optimize the channel power. Second, the tests are performed in a scenario with carriers that are distant from each other, with a frequency separation in GHz order.

MATERIAL AND METHODS

A radio frequency (RF) transmission signal can be represented by a real part of a complex baseband signal shifted to the carrier frequency. The carrier and the random phase of the carrier are constant. Thus, if the bandwidth of the baseband signal is much smaller than the carrier, then the PA behavior can be modeled by a baseband model [1,5,7,12]. In the scenario of multiple carriers, each channel is modeled by its own equation, but each output channel has inputs from other channels. For example, in a scenario of two channels, the output of channel 1 has information from input channel 1 and influences of input from channel 2 simultaneously.

Let $s(t)$ be the RF signal of two carriers

$$s(t) = \Re[x_1(t) \exp(j\omega_1 t) + x_2(t) \exp(j\omega_2 t)], \quad (1)$$

where x_1 and x_2 are the baseband signals of two carriers, respectively. The two-dimensional improved memory polynomial (2D-IMP) [18] models the PA or DPD behavior for both channels as follows

$$y_1(n) = \sum_{p=0}^{P-1} \sum_{m=0}^M h_{p,m}^{(1)} x_1(n-m) |x_1(n-m)|^p + \sum_{q=0}^{Q-1} \sum_{p=1}^{P-1} \sum_{m=0}^M h_{q,p,m}^{(1)} x_1(n-m) |x_1(n-m)|^q |x_2(n-m)|^p, \quad (2)$$

$$y_2(n) = \sum_{p=0}^{P-1} \sum_{m=0}^M h_{p,m}^{(2)} x_2(n-m) |x_2(n-m)|^p + \quad (3)$$

$$\sum_{q=0}^{Q-1} \sum_{p=1}^{P-1} \sum_{m=0}^M h_{q,p,m}^{(2)} x_2(n-m) |x_2(n-m)|^q |x_1(n-m)|^p,$$

where M is the memory length, P is the in-channel nonlinearity, Q is the concurrent channel nonlinearity interference, x_1 and x_2 are the input of the channels 1 and 2, y_1 and y_2 are the output of the channels 1 and 2, respectively, and h is the adjustable parameter. Due to the linearity in its parameters, each channel of the 2D-IMP model can be rewritten as a linear form of type

$$y(n) = x(n)\mathbf{h}, \quad (4)$$

where $y(n)$ is the output, $x(n)$ is a row vector that has all model inputs for time instant n , and \mathbf{h} is a column vector with adjustable coefficients. Due to the model linearity in its parameters, the vector \mathbf{h} can be extracted using a linear methodology, for example, the least squares (LS) [19] with two iterations of indirect learning architecture [20-21].

Dual-band transmission contextualization

This section revisits the mathematical description of the signal which is amplified by a concurrent dual-band PA. As shown by (1), the transmission signal has two envelopes for ω_1 and ω_2 carriers. Both carriers can be rewritten by an offset of a central carrier

$$\omega = \frac{\omega_1 + \omega_2}{2}, \quad (5)$$

thus, each carrier has an offset of $\Delta\omega$, where

$$\Delta\omega = \frac{\omega_2 - \omega_1}{2}. \quad (6)$$

Replacing ω_1 by $\omega - \Delta\omega$ and ω_2 by $\omega + \Delta\omega$, then (1) can be replaced by

$$s(t) = \Re[(x_1(t) \exp(-j\Delta\omega t) + x_2(t) \exp(j\Delta\omega t)) \exp(j\omega t)]. \quad (7)$$

Now, the complex envelope $x(t)$ carried by ω can be defined as

$$x(t) = x_1 \exp(-j\Delta\omega t) + x_2 \exp(j\Delta\omega t). \quad (8)$$

The complex envelope $x(t)$ centered in ω has contributions of $x_1(t)$ shifted from $-\Delta\omega$ and $x_2(t)$ shifted from $\Delta\omega$ in frequency. If both components of $x(t)$ have only dynamic contributions of x_1 and x_2 , being $\exp(-j\Delta\omega t)$ and $\exp(j\Delta\omega t)$ only frequency offsets, the dynamic contribution of $x(t)$ will also have only x_1 and x_2 dynamics. If the premise of dynamically is true, then the same sampling frequency f_s of x_1 and x_2 can be used to $x(t)$ without information lost. Soon

$$x(n) = x_1(n) \exp\left(-\frac{j\Delta\omega(n-1)}{f_s}\right) + x_2(n) \exp\left(\frac{j\Delta\omega(n-1)}{f_s}\right). \quad (9)$$

Some information is considered true at this moment. First, the generic envelope $x(t)$ can be subsampled at baseband f_s ; second, the mixers for x_1 and x_2 have the same phase alignment; and third, the mixer phases are constant and well known by the pre-distorter processor.

Saturation approach for dual-band transmission

A saturation methodology for single-band transmission has been introduced in [16] and improved in [17] including a phased treatment. The improvement needs to be used when the PA shows a phase change in a high suppression gain. However, for a low-phase change, the first version works well as expected. Applying the saturation in the general envelope $x(n)$ with amplitude L , the new signal $x_c(n)$ is

$$x_c(n) = \begin{cases} x(n), & \text{if } |x(n)| \leq L \\ L \exp j\angle x(n), & \text{if } |x(n)| > L \end{cases} \quad (10)$$

For one band transmission, after the saturation process, the signal $x_c(n)$ receives a distortion and a frequency offset to the transmission carrier. However, for two-band transmission, the distorter actuates only for x_1 or x_2 envelopes. Hence, the excess $|x(n)| - L$ pruned in $x_c(n)$ has to be imposed in x_1 and x_2 . In other words, $x_c(n)$ is composed of $x_{1c}(n)$ and $x_{2c}(n)$. In the following, two approaches will be introduced to have $x_{1c}(n)$ and $x_{2c}(n)$.

Sum approach

Let $z(n) = |x(n)| - L$ when $|x(n)| > L$. In the sum approach each channel applies the half part of the excedent keeping the original phase as

$$x_{1c}(n) = \left\{ \begin{array}{ll} x_1(n), & \text{if } |x(n)| \leq L \\ \left(|x_1(n)| - \frac{z(n)}{2} \right) \exp(j\angle x_1(n)), & \text{if } |x(n)| > L \end{array} \right\} \quad (11)$$

and

$$x_{2c}(n) = \left\{ \begin{array}{ll} x_2(n), & \text{if } |x(n)| \leq L \\ \left(|x_2(n)| - \frac{z(n)}{2} \right) \exp(j\angle x_2(n)), & \text{if } |x(n)| > L \end{array} \right\}. \quad (12)$$

Division approach

Let $z(n) = \frac{|x(n)|}{L}$, when $|x(n)| > L$. Then each channel envelope receives

$$x_{1c}(n) = \left\{ \begin{array}{ll} x_1(n), & \text{if } |x(n)| \leq L \\ \frac{x_1(n)}{z(n)}, & \text{if } |x(n)| > L \end{array} \right\} \quad (13)$$

and

$$x_{2c}(n) = \left\{ \begin{array}{ll} x_2(n), & \text{if } |x(n)| \leq L \\ \frac{x_2(n)}{z(n)}, & \text{if } |x(n)| > L \end{array} \right\}. \quad (14)$$

Whenever this approach is fulfilled, when $|x(n)| > L$ the signal reduces to $L \exp(j\angle x(n))$ as:

$$\frac{x_1(n)}{z(n)} + \frac{x_2(n)}{z(n)} = \frac{x(n)}{|x(n)|/L} = L \exp(j\angle x(n)). \quad (15)$$

The complete diagram implementing a saturation process for dual-band transmission is shown in Figure 1. The original signals to be transmitted, $x_1(n)$ and $x_2(n)$, are used to the Env block, responsible to get the general envelope around the mean carrier ω and sending the excedent $z(n)$. The Sat blocks implement the saturation to each band using one of the sum or division approaches. The resulting signals $x_{1c}(n)$ and $x_{2c}(n)$, which have the saturation implemented, are then distorted by the DPD block using the 2D-IMP as known in the literature resulting in $x'_{1c}(n)$ e $x'_{2c}(n)$ signals.

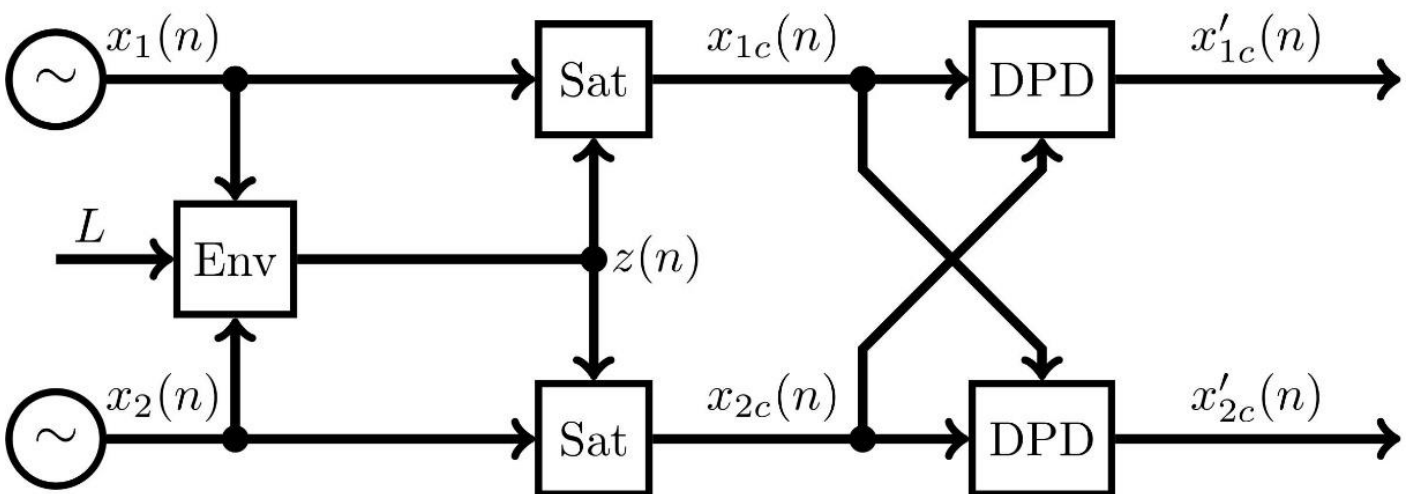


Figure 1. Implementation of DPD saturation for dual-band transmission.

Test setup and procedures

The linearization is done as follows. First, the PA was excited with two signals in a concurrent dual band. The input and output PA signals are collected in RF. After the demodulation process, a 2D-IMP behavioral model is implemented in baseband. Second, a traditional DPD for dual-band is used to distort the input PA signals. At this time, the PA is excited with a distorted signal and will present a behavior slightly modified. A new learning iteration with the current input and output signals allows the DPD to be more accurate. Thereafter, the system, DPD cascaded with the PA, will show the best linearity. This procedure is called indirect learning architecture [18,20-21]. Finally, the DPD saturation can be applied as shown in Figure 1.

For this work, the available device under test is a project of a broadband PA in the Cadence Virtuoso software detailed in [12]. This broadband PA can operate from 2 GHz up to 6 GHz, and can comply with IEEE 802.11n of 2.4 GHz and 5 GHz, as well as proprietary standards. For the dual-band transmission, signals of IEEE 802.11n at 2.4 GHz and Long Term Evolution (LTE) at 3.5 GHz standards were selected. Both are generated with Cadence Virtuoso with 20 MHz bandwidth, sampled with 120 MHz, and having 64-QAM constellation. The Matlab software is also available and used to perform the digital procedure.

Cadence Virtuoso does the signal generation, PA evaluation and measurement metrics such as error vector magnitude (EVM) and power spectral density (PSD) mask. Transient simulations in RF evaluate the PA behaviors due to the concurrent dual-band application. Text files apply the input signal and save the current and output voltages. The Matlab software is responsible for input signal generation, reading the output information, making the missing modulation blocks, DPD learning and implementation, and evaluating the power efficiency. The summarization of Cadence Virtuoso and Matlab interactions are shown in Figure 2. All interactions are done manually. In other words, features of each software for saving and reading text files are used. Then a new simulation is executed in Cadence Virtuoso, as well as a new script is executed in Matlab. Green blocks indicate a Cadence Virtuoso simulation. The Signal generation block indicates a wireless simulation using a communication standard and time results are saved as text files. The PA evaluation block is a transient simulation where the PA input signal is set to read a text file. The results of amplitude and currents are saved as text files to be read by Matlab. Finally, Cadence is also used for EVM metric generation using the standards settings. Matlab just implements the respective block instructions using a script. Note that, the first gray block is the first PA evaluation of indirect learning architecture; the second gray block needs to be repeated two times to concern with indirect learning architecture; the third gray block implements the introduced idea of this paper and creates data to get the evaluation metrics.

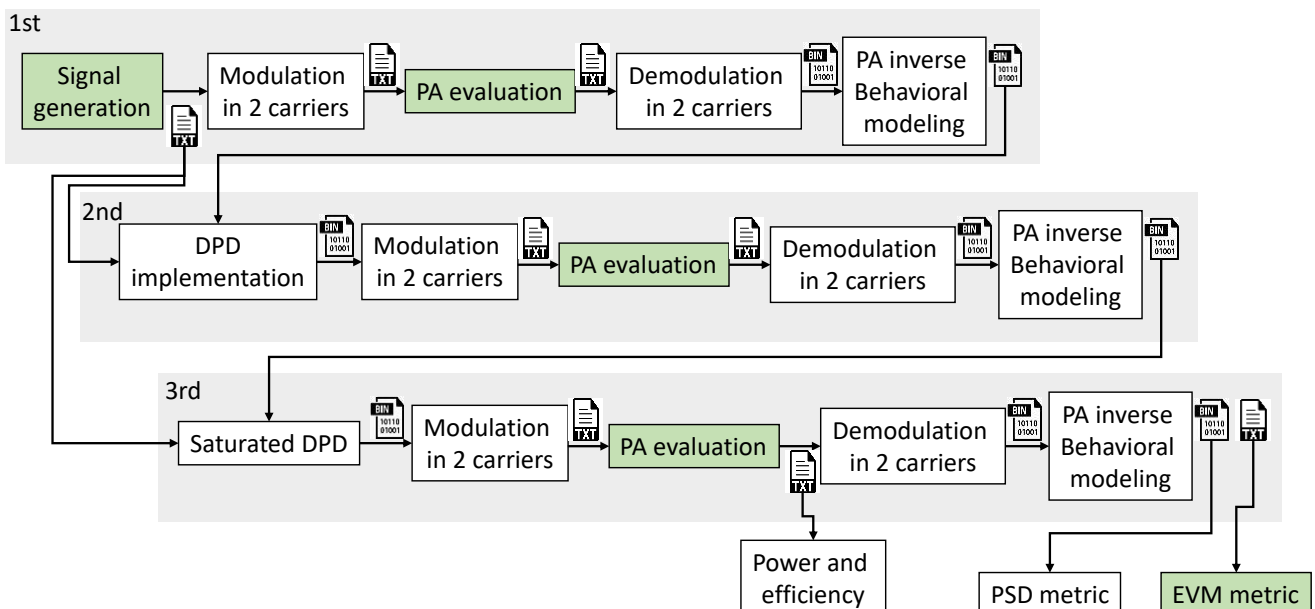


Figure 2. Block diagram of Matlab (in white blocks) and Cadence Virtuoso (green blocks) validation tasks.

RESULTS

This section shows the implemented tests according to the previous explanation. The first subsection shows the saturation of the global envelope and how it works in each band. The second subsection has the dual-band saturation applied to the linearization.

Dual-band saturation

Let $x_1(n)$ and $x_2(n)$ be the samples of ieee802.11n and LTE standards, respectively. The first 100 samples were normalized to have 1 V of maximum amplitude. Consequently, the maximum amplitude of $x(n)$ can be higher than 1 V. For carriers of 2.4 GHz and 3.5 GHz to x_1 and x_2 , respectively, the mean frequency is 2.95 GHz with a $\Delta\omega$ of $2\pi 550$ Mrad/s. Applying the saturation for $L = 1$ V into $x_1(n)$ and $x_2(n)$, the $x(n)$ and $x_c(n)$ responses are shown in Figures 2a and 2b for the sum and division approaches. The algorithm worked coherently, but the division option shown a better performance. Figures 4a and 4b show the amplitude by channel before and after the clipping process with the sum approach for the ieee802.11n and LTE channels, respectively. Whenever $|x(n)| > L$, x_1 and x_2 change abruptly. In the linearization procedure, the expected over- L parameter is smaller than the ones showed in Figure 3.

The main problem with the proposed approach is the extrapolation model. Constraints in the x_1 and x_2 envelopes do not guarantee the model boundaries because of the model memory length greater than zero. Consequently, the output model and the DPD implementation can show unexpected values.

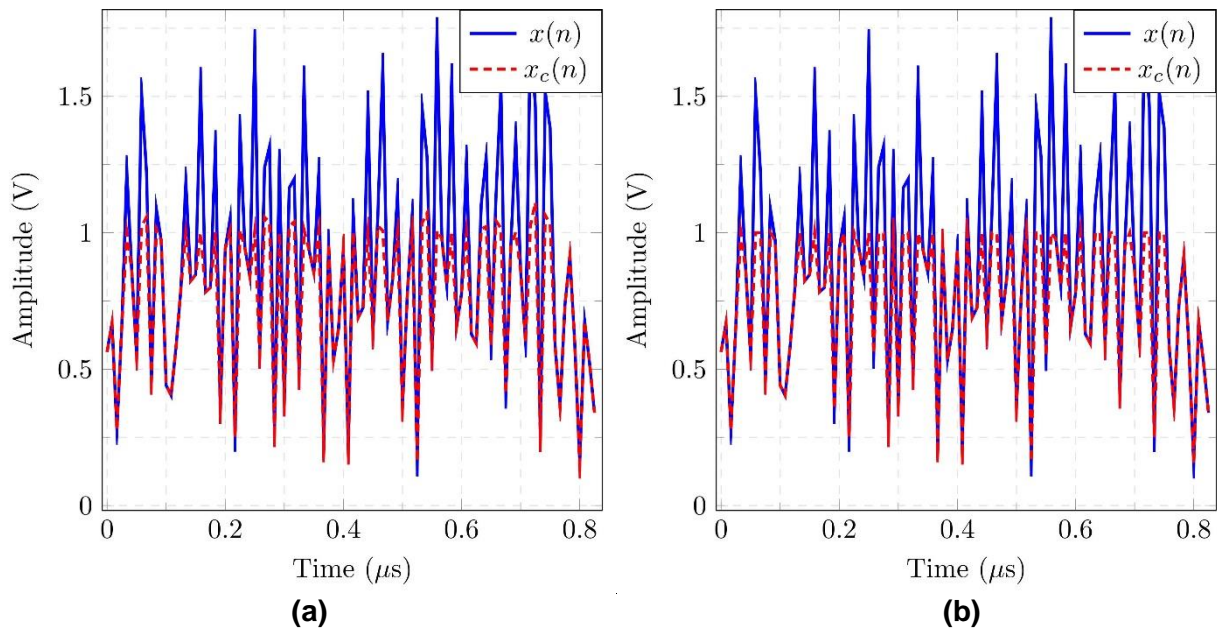


Figure 3. Amplitudes of $x(n)$ and $x_c(n)$ for $L = 1$ V using (a) the sum and (b) division approaches.

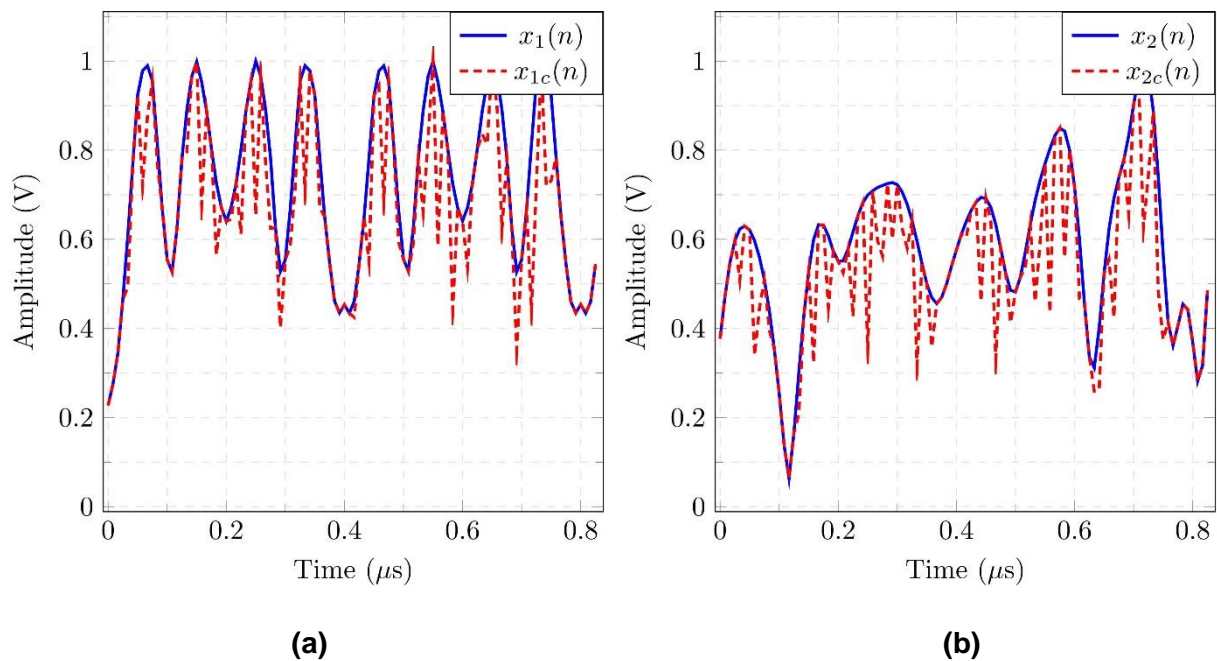


Figure 4. Amplitudes of sum approach for $L = 1$ V (a) channel 1 and (b) channel 2.

Linearization with dual-band saturation

The linearization test goal is to get the quantitative evaluation of how much the PA output power increases complying with the linearity requirements. The greater the PA output power, the greater the PA efficiency. Finally, the saturation must allow raising the output power even as keeping the EVM and PSD lower than without linearization.

The application of the saturation procedure is after the indirect learning second iteration. The maximum amplitude of traditional linearization defines the L value, and each channel admits the controlled overlapped signal. The main reason for individual channel control is power control independence.

For the overlap varying from 0 to 50%, Tables 1 and 2 display the main linearization metrics with sum and division approaches. Both have similar performances. The output mean power (Pout) increased less than 1 dB. However, the PAE changes widely, up to 17%, without a substantial loss in the EVM metric.

Table 1. Linearization performance results of concurrent dual-band with saturation using the sum approach.

Overlap	Pout (dBm)	PAE (%)	EVM Channel 1 (%)	EVM Channel 2 (%)
00%	20.86	14.7	1.17	1.23
10%	20.99	15.2	1.07	1.39
20%	21.13	15.7	1.49	2.08
30%	21.27	16.3	2.61	2.51
40%	21.42	16.9	5.03	4.02
50%	21.58	17.3	8.46	6.81

Table 2. Linearization performance results of concurrent dual-band with saturation using the division approach.

Overlap	Pout (dBm)	PAE (%)	EVM Channel 1 (%)	EVM Channel 2 (%)
00%	20.86	14.7	1.17	1.23
10%	20.99	15.2	1.07	1.39
20%	21.13	15.7	1.49	2.08
30%	21.27	16.3	2.64	2.53
40%	21.42	17.0	5.00	4.06
50%	21.58	17.3	8.24	6.78

Table 3 shows a comparison with the same output mean power. The 25% overlap attends the maximum EVM deterioration. Traditional linearization has output power smaller than others because of the maximum signal output. Figures 5a and 5b show the PSD of IEEE802.11n and LTE channels. The yellow line indicates the PSD constraint of the respective standards.

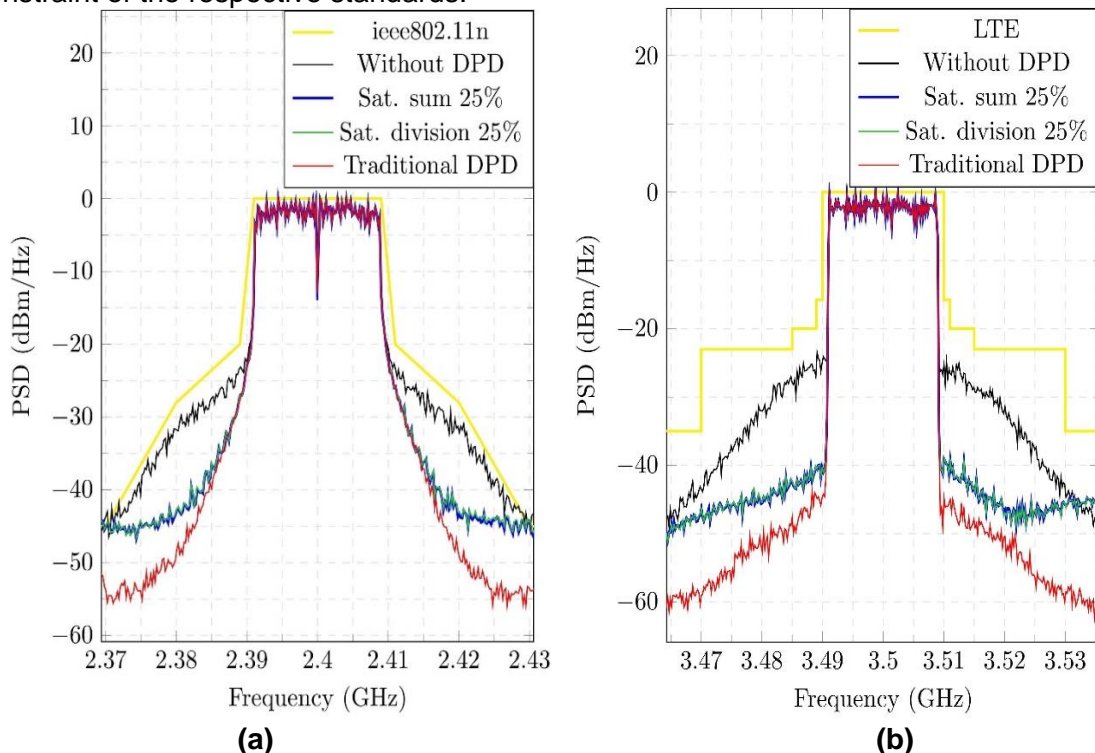


Figure 5. Power spectral density of PA output for (a) IEEE802.11n and (b) LTE channels.

Table 3. Comparison between traditional linearization, linearization with dual-band saturation, and without linearization.

Scenario	Pout (dBm)	PAE (%)	EVM Channel 1 (%)	EVM Channel 2 (%)
Without linearization	21.21	16.1	9.83	11.68
Sum with 25%	21.20	16.0	1.89	2.13
Division with 25%	21.20	16.0	1.89	2.14
Traditional linearization	20.86	14.7	1.17	1.23

The worst EVM without linearization indicates mandatory linearization. The EVM gain with linearization reaches 7.9 percentage points (p.p.) and 9.5 p.p. for IEEE802.11n and LTE channels. While literature linearization imposes limits on the power and PAE, the saturation introduced in this paper allows the PAE gain with a slight loss in the EVM metric. The efficiency gain achieves 8.8 p.p. for EVM loss of less than one p.p. Despite the low EVM deterioration, the PSD increased considerably but remained lower than the standard mask and lower than without linearization. Finally, comparing the sum and division approaches, both deliver similar performance. The sum approach offered a little better performance.

DISCUSSION

Radiofrequency transmitters should apply digital linearization to have efficiency and good performance. Traditional linearization limits the PA output power but allows the system to show higher linearity than mandatory. Literature introduces the DPD saturation to increase the power and the efficiency at the cost of losing the linearity for one carrier transmitter. The treatment for dual-band transmission with two approaches in this paper delivers the remaining output amplitude for each channel envelope. The DPD saturation with sum and division approaches allows a concurrent dual-band PA to increase the efficiency up to 8.8 p.p. in the PAE metric with EVM degradation of less than 1 p.p. and EVM reduction of about 9 p.p. when compared with the case without linearization.

This work introduced a mathematical approach based in carrier frequency and phase offset that allows the traditional DPD saturation to be applied for concurrent dual-band transmission. Suggestions for future research include the application in scenarios with more than two carriers and the distribution of the overlap amplitude for each band considering the band power. Analysis and treatment for model extrapolation is a missing development too.

Acknowledgments: The authors would like to thank the Aperfeiçoamento de pessoal de nível superior (CAPES) by part of funding and Conselho Nacional de Desenvolvimento Científico e Tecnológico (CNPq).

Conflicts of Interest The authors declare no conflict of interest.

REFERENCES

1. Manyam VN, Pham DKG, Jabbour C, Desgreys P. A low-power high-performance digital predistorter for wideband power amplifiers. *Analog Integr. Circuits Signal Process.* 2018;97(3):483-92.
2. Hasin MR, Kitchen J. A compact watt-level GaN-on-Si class AB power amplifier for handset applications. In: 2017 Texas symposium on Wireless and Microwave Circuits and Systems (WMCS). IEEE; 2017. p. 1-4.
3. Ackermann T, Potschka J, Maiwald T, Hagelauer A, Fischer G, Weigel R. A Robust Digital Predistortion Algorithm for 5G MIMO: Modeling a MIMO Scenario With Two Nonlinear MIMO Transmitters Including a Cross-Coupling Effect. *IEEE Microw. Mag.* 2020;21(7):54-62.
4. Mayeda J, Lie D, Lopez J. A highly efficient and linear 15 GHz GaN power amplifier design for 5G communications. In: 2017 Texas Symposium on Wireless and Microwave Circuits and Systems (WMCS). IEEE; 2017. p. 1-4.
5. Dardaillon M, Jabbour C, Srinivasa VP. Adaptive digital pre-distortion for future wireless transmitters. In: 2015 IEEE international conference on electronics, circuits, and systems (ICECS). IEEE; 2015. p. 332-335.
6. Wood J. Digital pre-distortion of RF power amplifiers: progress to date and future challenges. In: 2015 IEEE MTT-S International Microwave Symposium. IEEE; 2015. p. 1-3.
7. Cripps SC. RF power amplifiers for wireless communications. vol. 250. Artech house Norwood, MA; 2006.
8. Khawam Y, Albasha L, Mir H. Accurate and low complexity polynomial and neural network models for PA digital pre-distortion. In: 2016 16th Mediterranean Microwave Symposium (MMS). IEEE; 2016. p. 1-4.
9. Razavi B, Behzad R. RF microelectronics. vol. 2. Prentice hall New York; 2012.
10. Gilbert PL, Montoro G, Vegas D, Ruiz N, García JA. Digital predistorters go multidimensional: DPD for concurrent multiband envelope tracking and outphasing power amplifiers. *IEEE Microw. Mag.* 2019;20(5):50-61.
11. Li TW, Huang MY, Wang H. Millimeter-wave continuous-mode power amplifier for 5G MIMO applications. *IEEE Trans. Microw. Theory Tech.* 2019;67(7):3088-98.

12. Schuartz L, Silva RG, Hara AT, Mariano AA, Leite B, Lima EG. Concurrent Tri-band CMOS Power Amplifier Linearized by 3D Improved Memory Polynomial Digital Predistorter. *Circuits, Systems, Signal Process.* 2021;40:2176-208.
13. Shokair A, Beydoun A, Pham DKG, Jabbour C, Desgreys P. Wide band digital predistortion using iterative feedback decomposition. *Analog Integr, Circuits Signal Process.* 2019;100:93-108.
14. Naik G, Liu J, Park JMJ. Coexistence of wireless technologies in the 5 GHz bands: A survey of existing solutions and a roadmap for future research. *IEEE Commun. Surv. Tutor.* 2018;20(3):1777-98.
15. Peng X, Qiu X, Mu F. Digital harmonic canceling algorithm for power amplifiers based on nonlinear adaptive filter. *Prog. Electromagn. Res. M.* 2018;65:151-64.
16. Schuartz L, Santos EL, Leite B, Mariano AA, Lima EG. Traditional and saturated digital baseband predistorters for wireless transmitters. In: *Proceedings of the 33rd South Symposium on Microelectronics. 33rd South Symposium on Microelectronics*; 2018. p.93-6.
17. Schuartz L, Hara A, Leite B, Mariano AA, Lima EG. Saturated predistorter for efficiency improvement of a cmos pa for 3.5 ghz lte and wi-fi in 2.4 and 5 ghz. In: *Proceedings of the 34rd South Symposium on Microelectronics. 34rd South Symposium on Microelectronics*; 2019. p. 139-42.
18. Schuartz L, Freire LB, Hara AT, Mariano AA, Leite B, Lima EG. Modified indirect learning applied to neural network-based pre-distortion of a concurrent dual-band CMOS power amplifier. *Analog Integr. Circuits Signal Process.* 2021;106:277-92.
19. Mathews VJ, Sicuranza G. *Polynomial signal processing.* John Wiley & Sons, Inc.; 2000.
20. Eun C, Powers EJ. A new Volterra predistorter based on the indirect learning architecture. *IEEE Trans. Signal Process.* 1997;45(1):223-7.
21. Chavez JH, Machado CLR, Lolis LHA, de Lima EG. Optimal parameter identification for look-up table based band-limited memory polynomial model using direct and indirect learnings. *J. Integr. Circuits Syst.* 2018;13(2):1-6.
22. Wang S, Cao W, Hou R, Eriksson T. A digital predistortion for concurrent dual-band power amplifier linearization based on periodically nonuniform sampling theory. *IEEE Trans. Microw. Theory Tech.* 2021;70(1):466-75.
23. Gao Y, Yu C, Li S, Liu Y. A Dual-band Sample Selection Method for 2-Dimension Digital Predistortion. In: *2023 IEEE International Workshop on Electromagnetics: Applications and Student Innovation Competition (iWEM).* IEEE; 2023. p. 213-5.
24. Zhang M, Liu J, Zhu D, Quan X, Xu Q, Liu Y, et al. A Post-Correction Method for Terahertz Nonlinear Distortion with Dual-Band Carrier Aggregation. In: *2022 IEEE Globecom Workshops (GC Wkshps).* IEEE; 2022. p. 1784-9.
25. Changwei C, Qin K, Mei H, Tang B, Cao Y. Novel Sector Two-Dimensional Crest Factor Reduction Techniques for Performance Improvement in Dual-Band System. *IEEE Access.* 2020;8:108811-20.
26. Tang K, Huang H, Yu C, Wu Y, Jin Q, Gao J, et al. A novel two-dimensional crest factor reduction method based on concurrent output capacity of power amplifiers. *Microw. Opt. Technol. Lett.* 2021;63(3):835-9.
27. Gilabert PL, Pérez-Cisneros JR, Ren Z, Montoro G, Lavín MdINR, García JA. Digital Predistortion Linearization of a GaN HEMT Push-Pull Power Amplifier for Cable Applications with High Fractional Bandwidth. *IEEE Trans. Broadcast.* 2023.
28. Wesemann S, Du J, Viswanathan H. Energy efficient extreme MIMO: Design goals and directions. *IEEE Commun. Mag.* 2023.



© 2024 by the authors. Submitted for possible open access publication under the terms and conditions of the Creative Commons Attribution (CC BY) license (<https://creativecommons.org/licenses/by/4.0/>)